



Characterizing the river water quality in China: Recent progress and on-going challenges

Jiacong Huang^{a,*}, Yinjun Zhang^b, Haijian Bing^c, Jian Peng^{d,e}, Feifei Dong^f, Junfeng Gao^a, George B. Arhonditsis^{g,*}

^a Key Laboratory of Watershed Geographic Sciences, Nanjing Institute of Geography and Limnology, Chinese Academy of Sciences, 73 East Beijing Road, Nanjing, 210008, China

^b China National Environmental Monitoring Centre, 8(B) Dayangfang Beiyuan Road, Chaoyang District, Beijing, 100012, China

^c Key Laboratory of Mountain Surface Process and Ecological Regulation, Institute of Mountain Hazards and Environment, Chinese Academy of Sciences, 9, Block 4, Renminnanlu Road, Chengdu, 610041, China

^d Department of Remote Sensing, Helmholtz Centre for Environmental Research—UFZ, Permoserstrasse 15, 04318, Leipzig, Germany

^e Remote Sensing Centre for Earth System Research, Leipzig University, 04103, Leipzig, Germany

^f Institute of Groundwater and Earth Sciences, Jinan University, 601 Huangpu Avenue, Guangzhou, 510630, China

^g Ecological Modelling Laboratory, Department of Physical & Environmental Sciences, University of Toronto, Toronto, ON, M1C 1A4, Canada

ARTICLE INFO

Keywords:

River water quality
Urbanization
Watershed management
Eutrophication
Bayesian modelling

ABSTRACT

Food production systems, urbanization, and other anthropogenic activities dramatically alter natural hydrological and nutrient cycles, and are primarily responsible for water quality impairments in China's rivers. This study compiled a 16-year (2003–2018) dataset of river water quality (161,337 records from 2424 sites), watershed/landscape features, and meteorological conditions to investigate the spatial water quality patterns and underlying drivers of river impairment (defined as water quality worse than Class V according to China's Environmental Quality Standards for Surface Waters, GB3838-2002) at a national scale. Our analysis provided evidence of a distinct water quality improvement with a gradual decrease in the frequency of prevalence of anoxic conditions, an alleviation of the severity of heavy metal pollution, whereas the cultural eutrophication has only been moderately mitigated between 2003 and 2018. We also identified significant spatial variation with relatively poorer water quality in eastern China, where 17.2% of the sampling sites registered poor water quality conditions, compared with only 4.6% in western China. Total phosphorus (TP) and ammonia-nitrogen (NH₃-N) are collectively responsible for >85% of the identified incidences of impaired conditions. Bayesian modelling was used to delineate the most significant covariates of TP/NH₃-N riverine levels in six large river basins (Liao, Hai, Yellow, Yangtze, Huai, and Pearl). Water quality impairments are predominantly shaped by anthropogenic drivers (82.5% for TP, 79.5% for NH₃-N), whereas natural factors appear to play a secondary role (20.5% for TP, 17.5% for NH₃-N). Two indicator variables of urbanization (urban areal extent and nighttime light intensity) and farmland areal extent were the strongest predictors of riverine TP/NH₃-N levels and collectively accounted for most of the ambient nutrient variability. We concluded that there is still a long way to go in order to eradicate eutrophication and realize acceptable ecological conditions. The design of the remedial measures must be tailored to the site-specific landscape characteristics, meteorological conditions, and should also consider the increasing importance of non-point source pollution and internal nutrient loading.

1. Introduction

Global river network with an estimated length of 7562×10^3 km (Lehner et al., 2011), together with 1.42 million lakes (Messenger et al., 2016), plays an important role in water supply worldwide (Oki and

Kanae, 2006). Rivers represent the pathways for mass transport from land to lakes and oceans, and are largely responsible for meeting the societal needs for drinking water, irrigation, and hydropower (Grill et al., 2019; Lehner et al., 2011; Palmer and Ruhi, 2019). However, river ecosystems are globally experiencing considerable degradation due to a

* Corresponding authors.

E-mail addresses: jchuang@niglas.ac.cn (J. Huang), george.arhonditsis@utoronto.ca (G.B. Arhonditsis).

<https://doi.org/10.1016/j.watres.2021.117309>

Received 14 January 2021; Received in revised form 11 April 2021; Accepted 25 May 2021

Available online 29 May 2021

0043-1354/© 2021 Elsevier Ltd. All rights reserved.

multitude of stressors, including damming and water pollution (Lebreton et al., 2017; Maavara et al., 2020; Singh et al., 2019). Dam construction has resulted in 2.8 million dams worldwide that have substantially altered river connectivity and biogeochemical cycling (Lehner et al., 2011; Maavara et al., 2020, 2015). A global investigation on 12 million kilometers of rivers revealed that only 37% of rivers longer than 1000 km remain free flowing over their entire length owing to the increasing number of dams (Grill et al., 2019). Another threat to the integrity of river ecosystems is water pollution due to excessive nutrient loading (Chen et al., 2019; Jarvie et al., 2018), plastic debris (Lebreton et al., 2017), antibiotics (Li et al., 2018; Singh et al., 2019; Zhang et al., 2015) and other pollutants. As a consequence, nearly 80% of the world's population is potentially faced with elevated water security risks (Vörösmarty et al., 2010), and one in three people worldwide do not have access to safe drinking water, as reported by the Sustainable Development Goal (SDG) of the United Nations (United Nations, 2020).

China's rivers have been subjected to profound water quality impairments induced by the rapid and energy-intensive economic development over the past several decades (Chen et al., 2019). This water quality impairment is particularly disconcerting due to its potentially deleterious impacts on ~1.4 billion population. Estimates of pollutant inputs into China's rivers vary considerably and may be up to 2.8×10^7 tonnes of dissolved nitrogen, 3×10^6 tonnes of dissolved phosphorus (Chen et al., 2019), and nearly 2.5×10^4 tonnes of antibiotics per year (Zhang et al., 2015). A nationwide survey of 1935 sampling sites at China's rivers, lakes and reservoirs in 2018 revealed that 29% of them had poor water quality, i.e., worse than Class III according to China's Environmental Quality Standards for Surface Waters (GB3838-2002), and 6.7% of them had extremely poor water quality, i.e., worse than Class V (The Ministry of Ecology and Environment, 2020a). According to a study published in 2014, China's water pollution has been responsible for a shortage of 40 billion tonnes of water per year (Tao and Xin, 2014). Thus, addressing river water quality and freshwater security issues in China is widely recognized as one of the emerging imperatives during the 21st century.

To shed light on the water quality patterns and underlying mechanisms in China's rivers, numerous modelling studies of high-frequency data (Yang et al., 2019), mass transport and biogeochemical cycling (Wang et al., 2016; Xia et al., 2018), driver characterization (Powers et al., 2016; Wang et al., 2016), and assessment of future water quality trends (Qu and Kroeze, 2010) have been carried out for a wide range of river ecosystems. Based on an overview of the impacts of watershed landscape on river water quality in China (Table S1), we found that riverine nutrient over-enrichment are of particular concern owing to its causal linkages with cultural eutrophication (Strokal et al., 2016), while other pollutants (e.g., antibiotics and polycyclic aromatic hydrocarbons) are gradually receiving more attention (Li et al., 2006; Singh et al., 2019). Critical factors shaping river water quality are greatly diverse across geographical regions, including hydrological regimes mainly driven by precipitation (Strokal et al., 2016; Yi et al., 2017), watershed landscape features and anthropogenic activities, such as land use (Ding et al., 2016; Xiao et al., 2016) or wastewater treatment plants (WWTPs) (Singh et al., 2019). In the same context, the establishment of the relationships between river water quality and covariates that reflect the intensity of anthropogenic activities and watershed natural characteristics within a watershed context represents a critical next step in advancing our contemporary understanding of the large-scale water quality patterns and underlying drivers. This piece of information can help us to identify hot spots and hot moments of water quality impairments, and to optimize the design of restoration practices at a national scale.

To investigate the spatial water quality patterns and critical covariates of river impairment, we compiled 16-year (2003–2018) datasets of river water quality, watershed/landscape features (elevation, slope, land uses, nighttime light intensity, spatial distribution and treatment capacity of wastewater plants), and meteorological conditions at a

national scale. To the best of our knowledge, this is by far the most comprehensive dataset representing China's river water quality at a national scale. Our study first evaluates the river water quality in China in terms of the severity of cultural eutrophication (i.e., nutrient concentrations, hypoxia severity) and heavy metal pollution. We then develop Bayesian models to delineate the most significant covariates of water quality in six large (Liao, Hai, Yellow, Yangtze, Huai, and Pearl) river basins. Drawing upon the wide variability contained into our national dataset, the delineation of the relationships between water quality and critical covariates can enhance our understanding of river response to anthropogenic stressors within a watershed context.

2. Materials and methods

2.1. Study area and data

A recent study by Wang et al. (2019) estimated that there are more than 20,000 rivers with a catchment area larger than 100 km² in China's Ten River Basins (Fig. 1). To map water quality in China's rivers, we compiled the following national datasets:

2.1.1. River water quality

To capture the dynamics of China's river water quality, a monthly sampling program has been conducted at 2424 sampling sites (Fig. 1) by the Chinese National Environmental Monitoring Centre. The sampling program resulted in a large dataset of 161,337 monthly samples covering a 16-year (2003–2018) period. This dataset included twenty four (24) water quality variables listed as the environmental quality standards for surface water (GB 3838-2002), while our focus here was on dissolved oxygen (DO), chemical oxygen demand (COD), total phosphorus (TP), ammonia nitrogen (NH₃-N), and eight heavy metals including copper (Cu), zinc (Zn), selenium (Se), arsenic (As), mercury (Hg), cadmium (Cd), chromium (Cr), and lead (Pb).

2.1.2. Meteorological data

To obtain the local meteorological conditions over the spatial domain covered by the national stream network, we used the Chinese Meteorological Forcing Dataset (CMFD) which has a fine spatio-

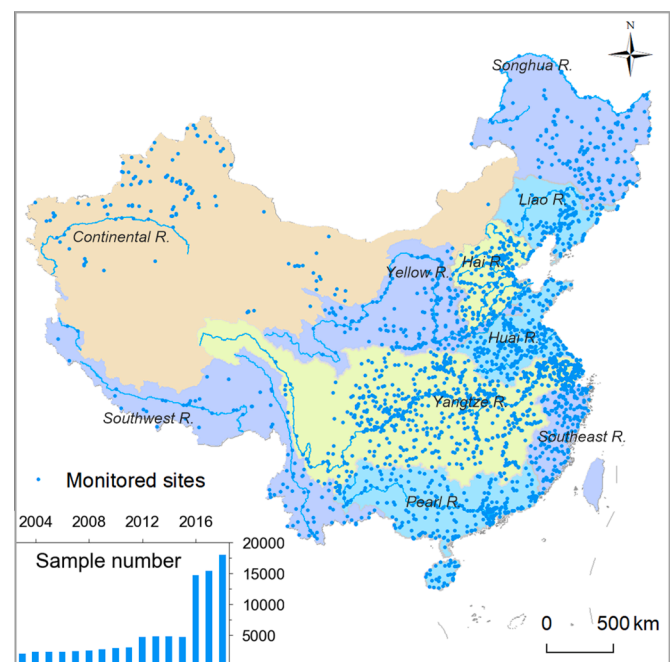


Fig. 1. Spatial and temporal information of the nationwide monitoring network in China's rivers during the 2003–2018 period.

temporal resolution with gridded near-surface meteorological data developed specifically for studies of land-surface processes across China (<http://data.tpdc.ac.cn/zh-hans/data/8028b944-daaa-4511-8769-965612652c49/>). The dataset has a spatial resolution of 0.1° , and includes information for seven variables: air temperature (T , $^\circ\text{C}$), pressure (Pa), specific humidity (kg/kg), wind speed (m/s), downward shortwave radiation (W/m^2), downward longwave radiation (W/m^2), and precipitation (Pr, mm/d) (He et al., 2020).

2.1.3. Watershed landscape data

The dataset includes elevation, slope, land use, nighttime light images, spatial distribution and water treatment capacity of WWTPs (Figure S1). Elevation was obtained from Shuttle Radar Topography Mission (SRTM), an international research effort to obtain global digital elevation models (<http://srtm.csi.cgiar.org/srtmdata/>). Slopes were derived from the elevation data. Land use data were obtained from the Resource and Environment Data Cloud Platform, Chinese Academy of Sciences (<http://www.resdc.cn/Default.aspx>). Nighttime light images were obtained from the NPP-VIIRS (the Visible Infrared Imaging Radiometer Suite (VIIRS) sensor on the Suomi National Polar-orbiting Partnership (NPP) Satellite) data by the National Oceanic and Atmospheric Administration (<https://www.ngdc.noaa.gov/eog/download.html>). The WWTP database across China were obtained from a previous study by Chen et al. (2019).

2.2. Characterization of river water quality and Bayesian modelling framework

We adopted a two-pronged approach to characterize the river water quality and potential drivers of impairment in China. First, based on the national river water quality dataset, we evaluated water quality status and identified the critical variables causing water quality deterioration using the Water Quality Index (WQI-DET) presented by Huang et al. (2019). Given the extensive water quality impairment attributed to TP and $\text{NH}_3\text{-N}$ (Section 3.2), Bayesian models were subsequently developed to examine the strength of the relationships between river TP/ $\text{NH}_3\text{-N}$ and watershed landscape features or surrogate variables of anthropogenic activities. Based on these Bayesian models, we used the posterior parameter patterns to characterize the critical covariates of river water

quality impairment in China (Fig. 2).

WQI-DET is an adaptation of the traditional WQI to the five water quality classes of China's "Environmental Quality Standards for Surface Water" (GB3838-2002): I (excellent), II (good), III (moderate), IV (poor) and V (bad) (Huang et al., 2019). The index can numerically represent a broader range from $-\infty$ (extremely poor water quality) to 100 (excellent water quality) in order to differentiate between bad and extremely bad water quality conditions. WQI-DET (WQI_{DET}^j) for a water sample j can be calculated as:

$$WQI_{DET}^j = \min(WQI_{DET-1}^j, \dots, WQI_{DET-i}^j, \dots, WQI_{DET-n}^j)$$

$$WQI_{DET-i}^j = 100 - \max\left(0, \frac{C_{ij} - C_i^I}{C_i^V - C_i^I} \times 100\right)$$

where C_{ij} is the concentration of the environmental variable i of the water sample j ; C_i^I and C_i^V are the values (concentrations) of the variable i at class I and V, respectively. Twelve (12) water quality variables were used to calculate WQI-DET, i.e., $n = 12$, and their concentrations were evaluated against the corresponding water quality classes (Table S2). We calculated a WQI-DET value for each of the 161,337 monthly water samples in the dataset.

We selected a total of 350 water quality sampling sites within six large river basins (Liao, Hai, Yellow, Yangtze, Huai, and Pearl) to elucidate the relative importance of watershed landscape characteristics and proxy variables of human-related activities on river water quality. The corresponding surrounding catchments were derived by the water flow directions computed by the D8 model in ArcGIS (Figure S2), and had a surface area ranging from 436 to 143,539 km^2 . These sub-watersheds were selected based on water flow pathways within the broader river basins, and were characterized by different meteorological/hydrological conditions, and socio-economic values. Sub-watersheds in lowland areas were not selected due to their reciprocating water flow paths which rendered unclear watershed boundaries. Based on the delineated sub-watershed boundaries, the data for the meteorological conditions, watershed landscape and anthropogenic activities for each sub-watershed were obtained to provide the predictor variables for our Bayesian modelling.

The first step of our water quality evaluation with WQI-DET revealed that water quality impairments was mainly caused by excessively high

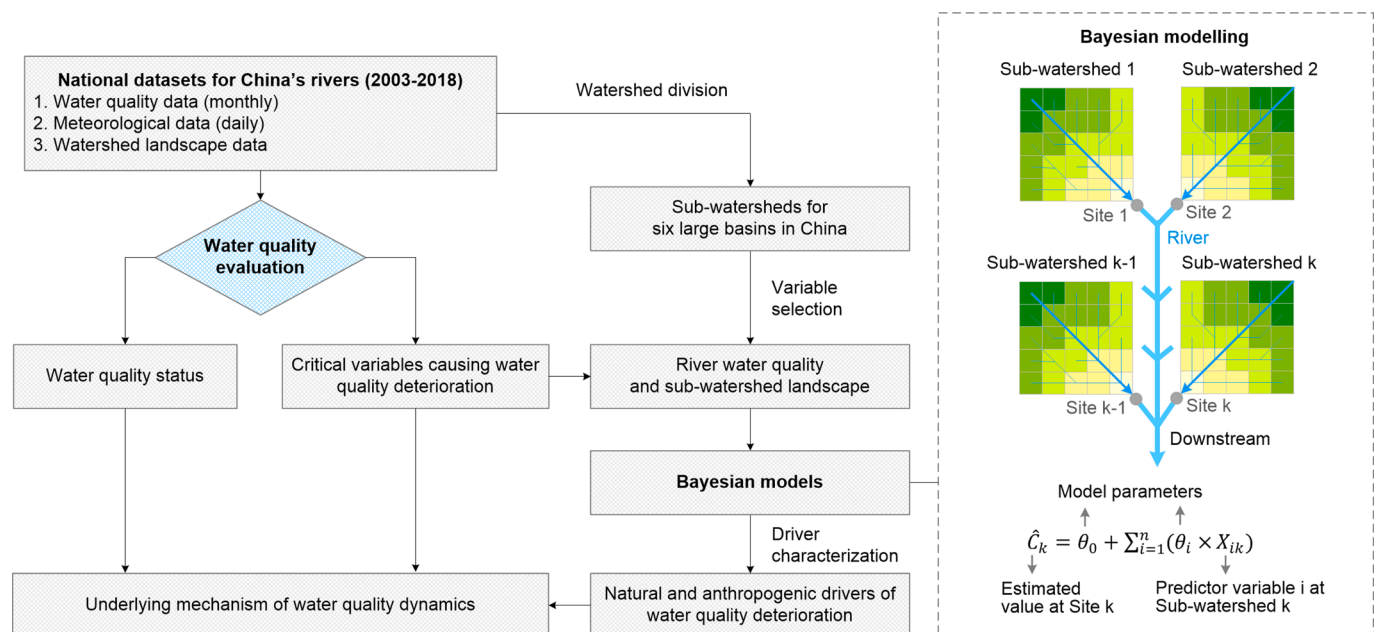


Fig. 2. Schematic illustration of our water quality evaluation framework and characterization of the dominant drivers of river water quality impairment in China using Bayesian modelling.

TP and NH₃-N concentrations (Section 3.2). The relationship between the two response variables (TP/NH₃-N) and natural or anthropogenic predictors was established through Bayesian modelling (Fig. 2). We developed a total of fourteen (14) Bayesian models including two national models for TP and NH₃-N collectively based on the water quality data at 350 sub-watersheds across six major river basins in China, and twelve models to reproduce TP and NH₃-N concentrations with suitable natural/anthropogenic predictors within each of six selected river basins independently. The governing equations of our Bayesian modelling framework can be summarized as follows:

$$\begin{aligned}
 C_k &\sim N(\hat{C}_k, \sigma^2) \\
 \hat{C}_k &= \theta_0 + \sum_{i=1}^N (\theta_i \times X_{ik}) \\
 \theta &\sim MN(\mu_\theta, \Sigma_\theta); \sigma^{-2} \sim G(0.001, 0.001) \\
 \mu_{\theta_i} &\sim N(0, 10000); \Sigma_\theta \sim IW(\Omega, \omega) \\
 k &= 1, \dots, K; i = 1, \dots, N
 \end{aligned}$$

where C_k denotes the measured TP or NH₃-N in site k within any of the modelled river basins (or the entire studied spatial domain), \hat{C}_k denotes the mean predicted TP or NH₃-N in site k , σ^2 denotes the model error variance with an associated precision (1/variance) term drawn from a Gamma (G) distribution defined by shape and scale parameters equal to 0.001; X_{ik} represents the predictor variables i in site k ; $\theta = [\theta_0, \theta_1, \dots, \theta_i]^T$ is the vector of the regression coefficients drawn from a multivariate normal (MN) distribution with mean $\mu_\theta = [\mu_{\theta_0}, \mu_{\theta_1}, \dots, \mu_{\theta_i}]^T$ and covariance matrix Σ_θ , which in turn is assigned an inverse-Wishart prior distribution with scale matrix Ω , representing an assessment of the magnitude order of the covariance matrix among the regression model parameters (Bouriga and Féron, 2013), $\omega (=8)$ corresponds to the degrees of freedom for this distribution and was set equal to the rank of the Σ_θ matrix (or no prior knowledge on the parameter covariance); $K (=350)$ and $N (=8)$ are the number of sites and predictor variables, respectively. Natural logarithm and arcsine square root transformations were used for both response and predictor variables to ensure that the assumption of normality for model residuals is met. The relative contribution W_i of each covariate X_i to TP and NH₃-N variability was calculated as follows:

$$\bar{\theta}_i = \left| \hat{\theta}_i \right| / \theta_{std}; W_i = \bar{\theta}_i / \sum_{i=1}^N \bar{\theta}_i$$

where $\bar{\theta}_i$, $\hat{\theta}_i$, and θ_{std} are the posterior standardized, mean, and standard deviation for the i regression coefficient, respectively.

The suite of predictor variables used to characterize river nutrient variations are classified into natural and anthropogenic variables. The natural predictors were *elevation* (m) and *slope* (°) to represent the natural conditions (e.g., transportation rates) with potential impacts on in-stream attenuation, *annual precipitation* (mm/yr) and *daily-average air temperature* (°C) to represent the potential impact of weather conditions on flow rates and biogeochemical processes. Our anthropogenic predictor variables were *area percentage of farmland and urban* (%) as a proxy of non-point source pollution, *water treatment capacity* of WWTPs (t/d/km²) to represent China's efforts to mitigate point-source pollution, *nighttime light intensity* to quantify the magnitude of human footprint. Compared with other proxy variables representing human footprint (e.g., population density), the nighttime light intensity had a finer spatio-temporal granularity and was thus deemed more suitable for our modelling analysis. We used the Mallows' C_p criterion to identify the most parsimonious regression models for each river basin and thus our analysis is based on statistical constructs that effectively balance between complexity and performance (Mallows, 2000). Moreover, as an additional security measure to control the collinearity problem, we ensured that the final models included predictor variables with

tolerance values greater than 0.5. Tolerance is defined as 1 minus the squared multiple correlation of this variable with all other independent variables in the regression equation. Therefore, the smaller the tolerance of a variable, the more redundant is its contribution to the regression (i.e., it is redundant with the contribution of other independent variables). If the tolerance of any of the variables in the regression equation is equal to zero (or very close to zero), then the regression equation cannot be evaluated (the matrix is ill-conditioned and cannot be inverted). Bayesian modelling was implemented based on the Python library of PyMC3 specifically developed for Bayesian statistical modelling and probabilistic machine learning (<https://docs.pymc.io/>). We also estimated the effective sampling size of the Markov chain Monte Carlo (MCMC) chains to assess the quality of the representation of the posterior distribution (higher values reflect better the posterior distribution of the parameters). We estimated the Gelman-Rubin index and the effective sampling size using the package coda in R (Plummer et al., 2006; Vehtari et al., 2020). The models performed adequately, showing convergence (all parameters with Gelman-Rubin estimate < 1.05) and low correlation in the MCMC chains samples (i.e., most parameters had an effective sample size > 1000).

3. Results

3.1. Characterization of river water quality impairment trends in China

Our results showed that China's river water quality displayed significant spatial variation with poorer water quality in eastern China (Fig. 3). Using the Hu Huanyong Line (Hu Line) to distinguish between western and eastern China, the frequency of poor water quality samples (WQI-DET < 40) was consistently higher in eastern China throughout our survey period (2003–2005, 2006–2010, 2011–2015, and 2016–2018). For example, 17.2% of the sampling sites showed poor water quality in eastern China, compared with only 4.6% in the western part of the country during the 2016–2018 period. Overall, our results are on par with the national evaluation by the Chinese Ministry of Ecology and Environment during the same period, which found that only 8.1% of sampling sites had extremely bad water quality, i.e., worse than Class V according to China's Environmental Quality Standards for Surface Waters (GB3838-2002) (The Ministry of Ecology and Environment, 2020a).

Among China's Ten River Basins, Hai and Huai River Basins had the poorest water quality with a similar median WQI-DET value of 61.8 in 2016–2018 (Fig. 3d), while the rest of the basins had WQI-DET values higher than 70. Water quality in Hai and Huai River Basins has significantly improved in recent years (2016–2018). Namely, the median WQI-DET value in Hai River Basin increased from −64.9 to 61.8 between 2003–2005 and 2016–2018. Likewise, Huai River Basin had a median WQI-DET value that increased from 46.1 to 61.8 in 2016–2018. Poor water quality mainly occurred in downstream areas, especially in coastal areas. In 2016–2018, we found 24.4% (30) of the 123 sampling sites in coastal areas (20 km buffer zone from the coastline) showed poor water quality. This proportion (24.4%) is significantly higher than that registered in western China (4.6%).

Six river basins (Songhua, Hai, Liao, Huai, Yellow, and Yangtze) showed a positive slope (k) ($p < 0.01$) for the trend line of the median WQI-DET values (Fig. 4), suggestive of a general water quality improvement during the 2003–2018 period. The general water quality improvement in China's rivers was also reinforced by another parallel comparison of sites that have been consistently sampled throughout the 2003–2018 study period (see Section 1 in Supporting Information). Hai River Basin was most severely polluted at the beginning of our study period with the lowest intercept (−70.7) for the trend line, but also showed significant water quality improvement with the highest slope ($k = 9.52$) or a 9.52 WQI-DET increase per year. Pearl River Basin showed a slightly decreasing trend ($k = -0.64$) of the median WQI-DET, but showed an increasing trend of the mean WQI-DET during 2003–2018. This implied that the overall water quality has not improved in Pearl

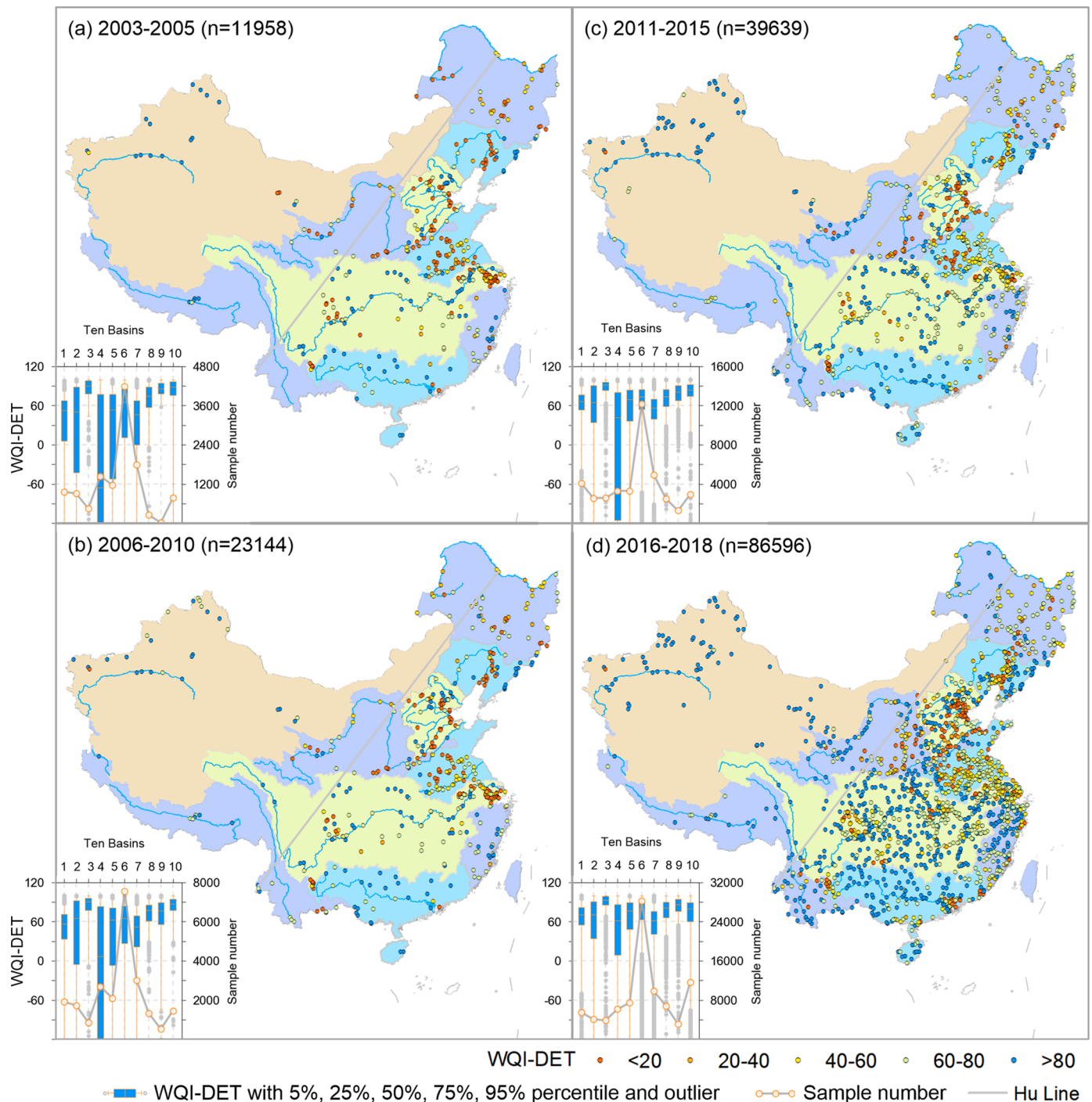


Fig. 3. Spatial patterns of water quality in China's rivers during the periods of 2003–2005, 2006–2010, 2011–2015, 2016–2018. Box-plots represent the WQI-DET distribution within China's Ten River Basins. 1–10 in X axes represent Songhua, Liao, Continental, Hai, Yellow, Yangtze, Huai, Southeast, Southwest, Pearl Rivers. WQI-DET represents a modification of the Water Quality Index (Huang et al., 2019). n is the number of data records.

River Basin, but the frequency of extremely poor water quality (extremely low WQI-DET) samples is decreasing. For visualization purposes, the extremely WQI-DET values (<-1000) were omitted from the corresponding panel in Fig. 4, but their influence is manifested with the significant discrepancy between average and median values. Three river basins (Southwest, Southeast, and Continental) did not show a clear changing pattern ($p>0.05$), but their water quality is relatively satisfactory.

A clear pattern of decreasing WQI-DET trend ($p<0.01$) from upstream to downstream sites was also found in Yellow and Yangtze

Rivers. In particular, water quality in Yangtze River displayed a discernible decline between the middle and downstream areas (Yichang-Shanghai) (Fig. 5). Liao, Hai, and Huai Rivers did not show a clear changing pattern ($p>0.05$) probably due to their high population density throughout the corresponding catchments areas. Interestingly, Pearl River showed relatively poor water quality at the upstream sites, followed by a gradual water quality improvement downstream. However, three sites near the city of Wuzhou displayed low WQI-DET values due to excessively high Hg concentrations in April of 2018 (Fig. 5), but the signature of this elevated Hg incident dissipated downstream of the

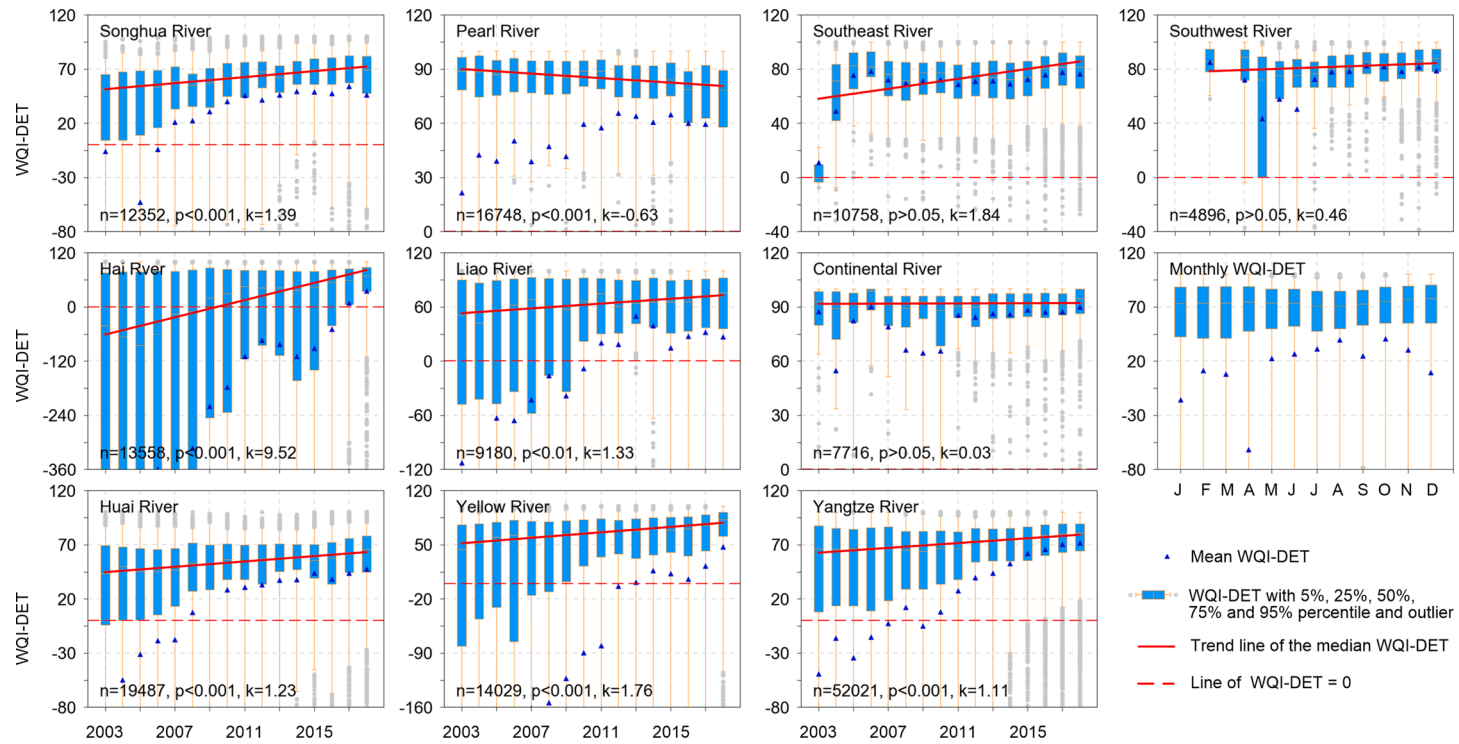


Fig. 4. Inter- and intra-annual variability of the WQI-DET values for China's Ten River Basins during the 2003–2018 period. n is the total sample size, p and k slope values for the trend lines are also provided.

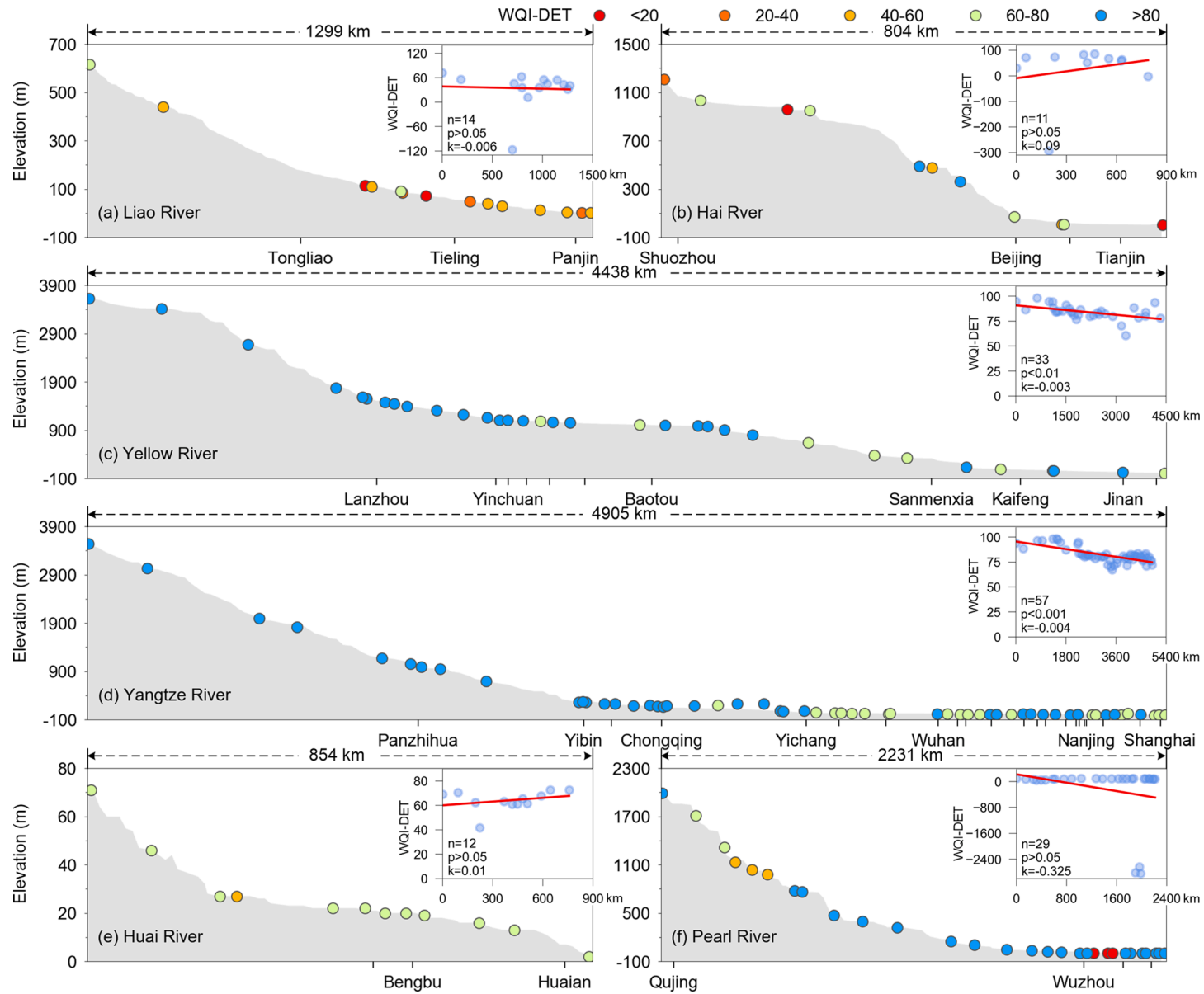


Fig. 5. Water quality along the Liao (a), Hai (b), Yellow (c), Yangtze (d), Huai (e) and Pearl (f) rivers during the 2016–2018 period. Several large cities along the rivers are labelled in the X axes. A scatter plot with a trend line (red colour) represents the WQI-DET trend from upstream to downstream. (For interpretation of the references to colour in this figure legend, the reader is referred to the web version of this article.)

three sites.

The absolute number of water samples indicative of impaired conditions ($WQI-DET < 0$) showed a slightly decreasing trend from 2003 to 2015, but had an abrupt increase from 2016 and thereafter, mainly stemming from the increased number of samples collected (Fig. 6a).

Evidence of impaired water quality conditions was found in 30.6% (741/2424) of all the sampling sites across China's rivers. In a similar manner, we used the relative frequency that each variable resulted in negative $WQI-DET$ values to identify the most sensitive indicators of water quality impairment in China's rivers during the 2003–2018

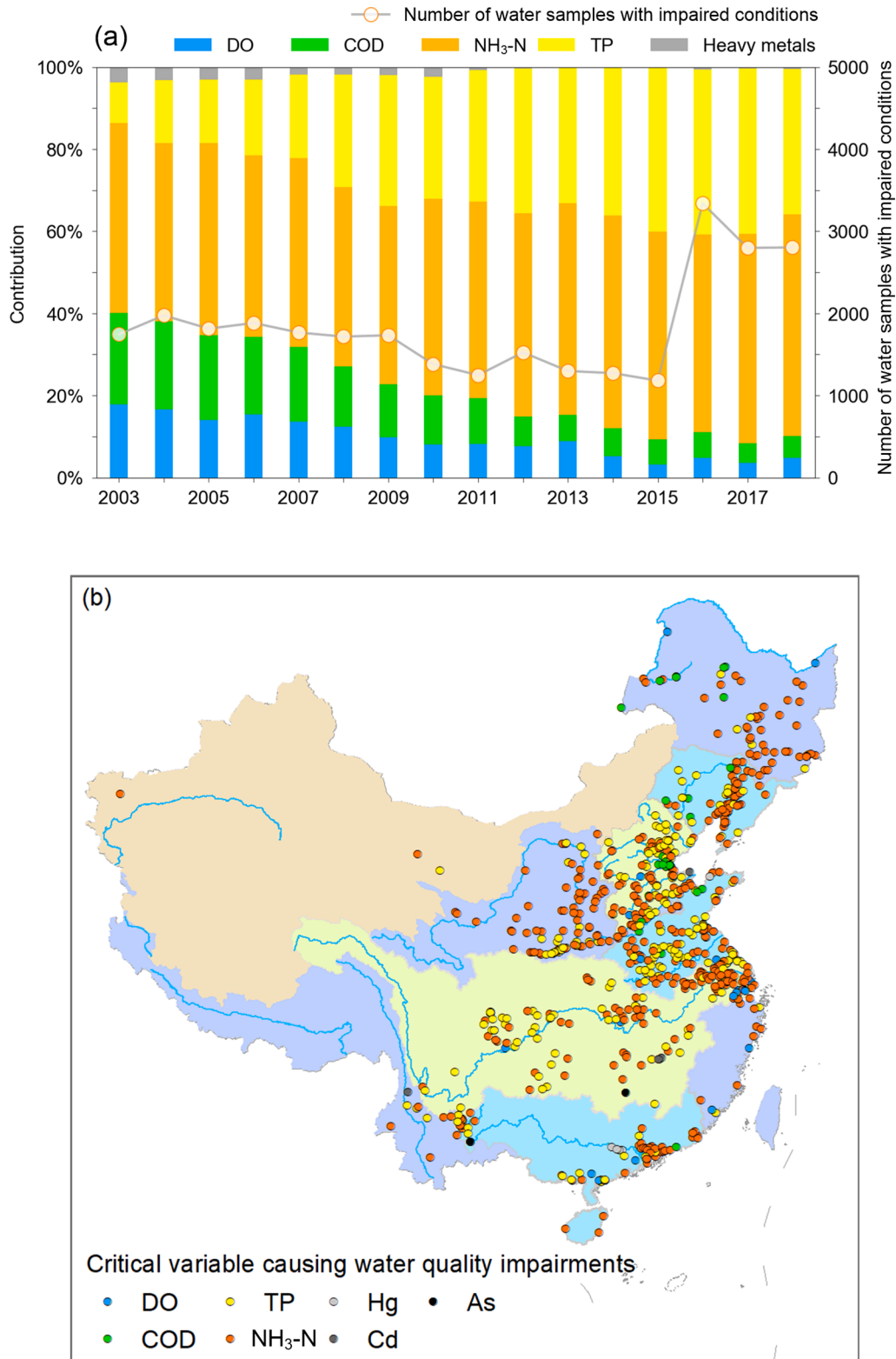


Fig. 6. Critical variables associated with water quality impairment in China's rivers: (a) Time-series contribution during 2003–2018 and (b) spatial distribution during 2016–2018. The contribution value for each variable was calculated by $n_{DET}^i / \sum_{i=1}^m n_{DET}^i$, where n_{DET}^i is the number of samples with a $WQI-DET$ value lower than 0 for the i variable, and m ($=12$) is the total number of water quality variables considered.

period. Our results revealed a decreasing contribution of variables reflecting either the bioavailable oxygen (DO) or the amount that can be consumed by reactions (COD), a fairly constant relative frequency of elevated $\text{NH}_3\text{-N}$, an increasing TP contribution to water quality impairment, and a very small proportion of HM pollution (Fig. 6a). The decreasing proportion from 17.9% (DO) and 22.2% (COD) in 2003 to 4.8% (DO) and 5.3% (COD) in 2018 collectively offers a more optimistic perspective regarding the habitat suitability for a diverse range of biotic

communities. In fact, only 20 sampling sites registered samples that reflected impaired water quality conditions due to DO, all located near large cities. Moreover, there was a very low percentage ($<0.3\%$) of severe HM (Hg, As, Cd, Pb and Se) pollution recorded in 14 sampling sites during the end of our study period.

In stark contrast, water quality impairment is primarily associated with elevated TP and $\text{NH}_3\text{-N}$ concentrations (Fig. 6b). Among the 741 sampling sites with impaired conditions, 648 sites registered excessively

(a)

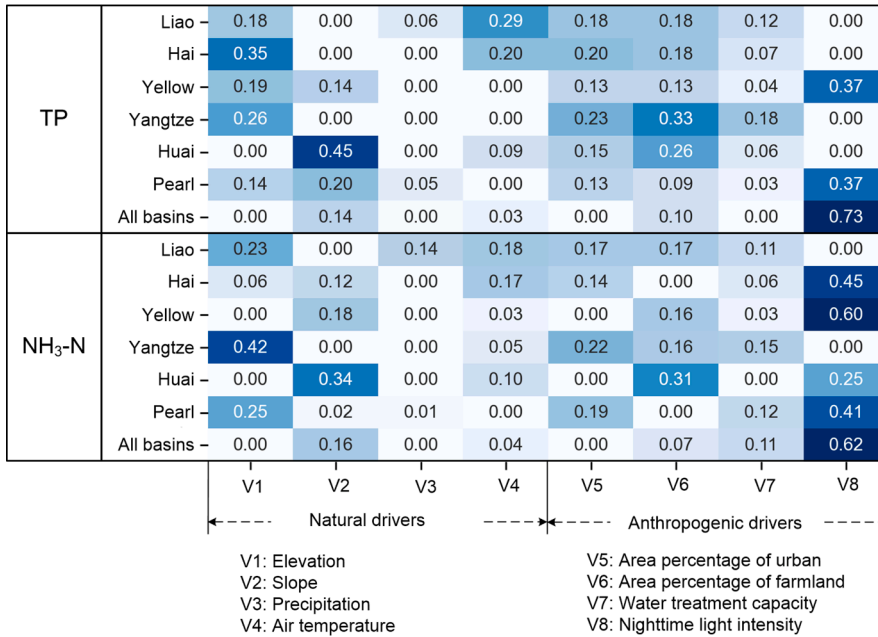
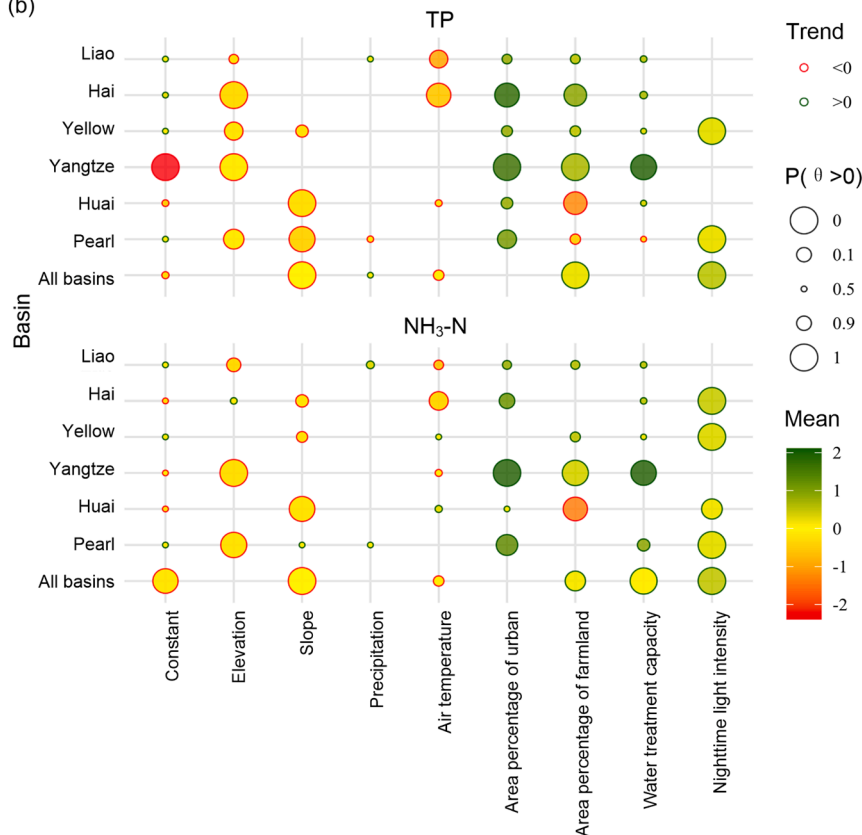


Fig. 7. Evaluation of the effects and percentage contribution of natural and anthropogenic drivers to the TP and $\text{NH}_3\text{-N}$ variability at six major rivers (Liao, Hai, Yellow, Yangtze, Huai, and Pearl) in China (a). For every predictor and river in (b), each circle represents the trend, mean, and probability of the slope being greater than zero, as derived from the posterior distribution of the slopes. The edge colour of each circle represents the trend of the mean value (positive or negative). The colour indicates the mean of the posterior distribution. Larger circles indicate that the probability of the slopes being positive is very high (slope is likely positive) or very low (slope is likely negative). (For interpretation of the references to colour in this figure legend, the reader is referred to the web version of this article.)

(b)



high TP/NH₃-N levels. TP showed an increasing proportion from 9.86% in 2003 to 35.4% in 2018. In terms of the actual TP concentrations, our analysis did not reveal distinctly declining trends, except from the Liao and Yangtze River Basins (Figure S3). In fact, the vast majority of the Ten River Basins frequently displayed high TP concentrations (>0.1 mg/L) during the 2016–2018 period. Evidence of statistically significant reduction in NH₃-N levels was found in Songhua, Hai, Huai, Yellow, and Yangtze River Basins, but high concentrations (>0.5 mg NH₃-N/L) continue to register with high frequency across all the major river basins (Figure S4). Overall, our attempt to characterize the river water quality in China provided evidence that TP and NH₃-N are collectively responsible for >85% of the identified incidences of impaired water quality in recent years (2016–2018).

3.2. Covariates of nutrient variability in China's rivers

Comparison between measured and predicted values along the six large rivers (Liao, Hai, Yellow, Yangtze, Huai, and Pearl) showed that our Bayesian models were generally able to recreate both TP and NH₃-N concentrations with $p < 0.01$ and low predictive bias (Figures S5 and S6). Among the covariates considered, the anthropogenic predictors had a larger contribution (82.5% for TP, and 79.5% for NH₃-N) compared with natural drivers (20.5% for TP and 17.5% for NH₃-N) when pooling the data from all six river basins together (Fig. 7a). Moreover, the posterior regression coefficients related to anthropogenic drivers had distinctly lower coefficients of variation compared with those for the natural drivers, which is suggestive of a higher degree of identification (low uncertainty) of the corresponding relationships with TP/NH₃-N concentrations (Table S3). Among the four selected natural drivers, elevation displayed a discernible contribution to nutrient variability, ranging anywhere from 6% to 42%, with only exception being the Huai River. In the latter basin, slope appeared to be the strongest covariate of riverine TP and NH₃-N levels. By contrast, precipitation and (less so) air temperature were weak predictors for both TP and NH₃-N concentrations across the six studied basins.

Regarding the selected anthropogenic drivers, our analysis showed that the percentage of farmland and urban area, and nighttime light intensity were critical covariates for TP and NH₃-N riverine levels (Fig. 7b; Table S3). The urban areal extent within any given watershed showed a consistently positive relationship with the two nutrient concentrations. The same pattern held true for the farmland area, except from the Huai River, where this relationship displayed a counterintuitive negative sign. Water treatment capacity had the lowest contribution (average value < 10%) to both TP and NH₃-N variability, except from the Yangtze River Basin, where a somewhat higher contribution (>15%) was registered (Fig. 7a). Interestingly, the nighttime light intensity had a distinct signature (>35%) on the two nutrient levels in Yellow and Pearl River Basins, as well as in all 350 sub-watersheds (72.9% and 61.6% for TP and NH₃-N) when pooled together (Fig. 7a). The latter result is reinforced by the spatial variability of the water quality impairments, where several “hot spots” of poor water quality were registered in four highly urbanized areas; namely, Beijing-Tianjin, Nanjing-Shanghai, Kunming, Shenyang (yellow and red colors in Fig. 8a). By contrast, sampling sites close to cities in central or western China (e.g., Lanzhou) with lower population density did not register severe water quality impairments. The spatial pattern of water quality bears a great deal of resemblance to that of average nighttime light intensity during 2016–2018, with high values of the latter predictor variable representing higher population size and density (Fig. 8b).

4. Discussion

Food security, urbanization, environmental degradation, and climate change are major challenges facing China in the 21st century. Being the largest developing country, China has experienced fast transition from centrally planned to market-orientated economy during the past three

decades, which was accompanied by rapid urbanization and major land-use conversion (Liu et al., 2014). Striving to achieve a food-production increase by 30–50% to meet projected demands, agriculture is increasingly intensified which has caused adverse environmental impacts and widespread degradation of surface waters (Cui et al., 2018; Liu and Li, 2017). To alleviate the pressure exerted from point- and non-point sources, China has taken remedial measures to restore its precious freshwater sources. Consequently, the construction of wastewater treatment plants has grown rapidly resulting in an increase from 40% to 90% of municipal wastewater being treated on the national scale within a time span of just over a decade (Tong et al., 2020; Zhou et al., 2018). On the other hand, tackling the problem of excess non-point nutrient sources by reducing fertilizer application rates and implementing watershed beneficial management practices has had less clear results (Liu et al., 2016). Even more so, little work has been done to evaluate the impact of all these remedial measures on the water quality of rivers at a national scale. In this context, the present study compiled a 16-year dataset of river water quality, meteorological conditions, and variables related to anthropogenic activities/landscape features to evaluate the degree of success brought about by all the recent efforts to combat water pollution.

4.1. How do anthropogenic factors and natural characteristics covary with China's river water quality?

Our attempt to characterize the signature of anthropogenic activities required to parse out the role of natural factors, such as meteorological conditions and landscape characteristics, in shaping riverine water quality. When considering all 350 sub-watersheds across China, our analysis was able to discern a weakly negative relationship between elevation and/or slope and TP/NH₃-N concentrations (Figure S7), suggesting that sites in higher elevations and/or steeper slopes registered lower nutrient levels. The slope of the catchment determines the water velocity and erosion severity, whereby mountainous rivers with higher slopes are expected to be subjected to faster flow velocities and more severe erosion, and thus shorter water retention times compared with lowland rivers (Palmer and Ruhi, 2019). However, our analysis did not render universal support to the latter hypothesis, partly due to the confounding effects of anthropogenic drivers that tend to negatively covary with the catchment elevation or slope (Figures S7–S8). Namely, lowland (low-slope) catchment areas are generally more urbanized with higher nutrient export (Figure S8). It is important to note though that the impacts of slope on water quality can also be influenced by the increasing number of dams in China, due to their considerable capability to modulate nutrient retention (Maavara et al., 2015).

Precipitation can determine the amount of inflowing water via surface and subsurface processes from urban areas or farmlands, and may thus significantly modulate the degree of nutrient loading from non-point sources (Stockwell et al., 2020). Recent research has shown that both particulate and bioavailable phosphorus loads can vary by orders of magnitude between wet and dry conditions (Long et al., 2014, 2015). Emerging evidence also suggests that a significant fraction of the annual phosphorus loads can be generated during a small number of brief but intense precipitation events. While the association of phosphorus with stormwater is plausible, the flow-concentration relationship can be profoundly modulated by factors such as watershed physiography, land use patterns, and antecedent conditions (Green et al., 2007). An overarching precipitation-concentration paradigm for nitrogen species is even less clear relative to that for phosphorus, given that a greater proportion of total nitrogen is found in the dissolved phase due to relatively high solubility of nitrogen species, such as nitrite and nitrate, and can be transported by subsurface and groundwater flow pathways (Long et al., 2014). Our expectation of a positive association between TP/NH₃-N and precipitation manifested itself only in Liao River (Table S3). This is because precipitation is highly correlated to elevation with a correlation coefficient of -0.99 (Figure S8). Therefore, elevation

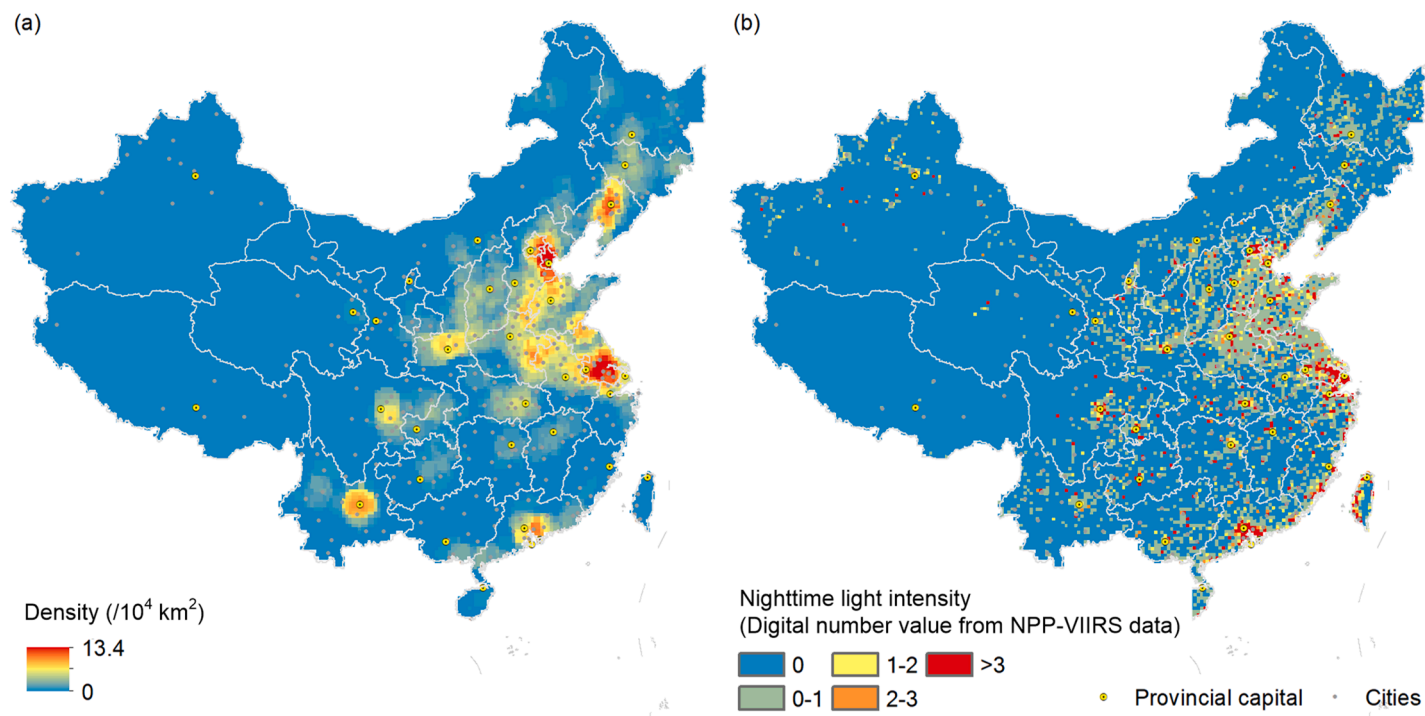


Fig. 8. Spatial variability of water quality impairment caused by TP and $\text{NH}_3\text{-N}$ in China's rivers (a), and nighttime light intensity (b) during 2016–2018. The left panel visualizes the density ($/10^4 \text{ km}^2$) of the sampling sites with registered water quality impairment. A value of 1 reflects that there is one site with water quality impairment over an area of 10^4 km^2 .

was selected as a covariate for the riverine nutrient levels, instead of precipitation. Similarly, air temperature can directly influence riverine thermal regimes and biogeochemical processes, such as nitrification, denitrification, ammonification, and sediment diagenesis rates (van Vliet et al., 2013; Xia et al., 2018; Yang et al., 2020). Although existing evidence suggests warmer temperatures result in higher recycling rates, and consequently higher nutrient retention in rivers (Xia et al., 2018), our analysis was not able to fully disentangle the temperature control on the ambient TP/NH₃-N levels, given its covariance with other natural or anthropogenic predictor variables (Figures S7-S8).

Counter to the relatively minor role of the natural factors considered in our analysis, the nighttime light intensity and the percentage of the urban area were the strongest predictors of riverine TP/NH₃-N levels and collectively accounted for most of the nutrient variability registered in the study sites. These distinctly positive relationships across all the major subwatersheds could reflect the influence of a suite of factors associated with the urban environment, such as inefficient stormwater management, suboptimal operating WWTP performance, underdeveloped sewers and sludge disposal facilities (Jiang et al., 2018; Qu et al., 2019). In particular, sustainable urban stormwater management is one of China's emerging challenges, where the infrastructural investments have not been on par with the continuous population growth, rapid urbanization, and socio-economic development. Taken together with the changing weather patterns and climate, the urban pluvial flooding gradually becomes a regular hydrometeorological phenomenon that has repeatedly affected many megacities in China (Du et al., 2015a, 2015b; Liu and Wang, 2016). To address the broader impact of the on-going urbanization and development process, the Chinese government has established a national initiative termed *sponge cities* as a holistic strategy that combines innovative technologies, effective governance, and broader community engagement to bring sustainable stormwater management into fruition (Jiang et al., 2018).

Water treatment capacity of WWTPs was another predictor considered to reproduce of the riverine nutrient variability. The rationale behind the selection of this covariate reflected China's efforts in building municipal WWTPs (>5000), and enforce more stringent effluent discharge standards during the past decades (Huang et al., 2019; The Ministry of Ecology and Environment, 2020b). China may have now the world's largest municipal wastewater infrastructure with a daily treatment capacity of nearly 200 million m³/d and a wastewater treatment ratio of over 90% (Qu et al., 2019). However, our analysis suggests a positive covariance between TP/NH₃-N and WWTP treatment capacity (Table S3). While this finding simply suggests the WWTP treatment capacity may not be the most sensitive variable to recreate the recent riverine nutrient trends, it could also reflect the fact that there are still considerable gaps in the design principles and operation performances of the treatment facilities, lagged development of sewer systems, disparity between the effluent discharge standards and the local conditions and environmental protection demands, and lack of appropriate sludge disposal (Qu et al., 2019). Viewed from this perspective, the water treatment capacity of WWTPs alone is not sufficient to predict the response of riverine ecosystems, and thus other surrogate variables of the urban environment (percentage urban area, nighttime light intensity) displayed stronger covariance with the water quality.

Non-point source pollution from agriculture has been widely recognized as a critically important source of nutrients into surface waters due to intensive fertilization. China's crop production maintained an average P fertilization rate of 80 kg/ha in 2012, which was twice as high as what crops can assimilate (Liu et al., 2016). Recognizing the challenges to accurately estimate the magnitude of non-point source pollution (Ongley et al., 2010; Shen et al., 2012), we postulated that the area percentage of farmland could display a discernible positive covariance with riverine TP/NH₃-N concentrations. Although our proxy of non-point source pollution from agriculture did not consistently register a distinct signature across the six river basins studied, it does support our hypothesis when pooling all the watersheds together (Fig. 7b). Even

though significant progress has been made in terms of the N and P loading export from agriculture (farming, aquaculture, livestock and poultry) between 2007 (1.598×10^9 kg TN and 1.087×10^8 kg TP) and 2017 (7.195×10^8 kg TN and 7.62×10^7 kg TP) (The Ministry of Ecology and Environment, 2020b), there is still a lot of grounds to cover in order to effectively mitigate non-point source pollution. To further address this issue, there are recommendations for a more efficient paradigm with P fertilizer management to address the dual challenge of P resource conservation and eutrophication mitigation, which will sustain future food production and maintain the integrity of freshwater ecosystems (Liu et al., 2016). In particular, it has been argued that China could delay exhausting its P reserves by over 20 years by improving its agronomic P use efficiency (defined as the ratio of the useful P output in products to the total P inputs in an ecosystem) to the average level of 80% in developed countries without any major implications for the targeted crop yields (Withers et al., 2014).

4.2. Challenges and on-going research questions with the river water quality management in China

Our study provided evidence of a distinct water quality improvement in China's major rivers with a gradual decrease in the frequency of prevalence of anoxic conditions, an alleviation of the severity of heavy metal pollution, and moderate success with the mitigation of cultural eutrophication during the 2003–2018 period. We also identified significant spatial variation with relatively poorer water quality in eastern China, nearby the major metropolitan areas of Beijing-Tianjin, Nanjing-Shanghai, Kunming, and Shenyang. The fact that more than 85% of the identified incidences of impaired conditions are associated with high nutrient concentrations suggests that our efforts to control point- and non-point source pollution should be further intensified. Notwithstanding the significant progress of China's wastewater treatment plant sector, the ubiquitous problems of the existing infrastructure (underdeveloped sewers and sludge disposal facilities, low sustainability of the treatment processes, mismatch between effluent discharge standards and environmental protection demands) represent one of the next management priorities. With the increasing prevalence of agricultural non-point source pollution, Best Management Practices (BMPs) are an emerging imperative in our efforts to prevent or reduce water pollution. Founded upon the pollution control theory of "source reduction–interception–repair", BMPs are increasingly applied in China's agricultural lands to mitigate non-point source pollution and restore aquatic ecosystems with variant results. Nonetheless, the design of BMPs should accommodate recent conceptual and technical advancements regarding the life-cycle non-stationarity, the variability in their starting operational efficiency, differential response to storm events or seasonality, dependence of operational performance on watershed geological conditions, and expected decline in performance over time owing to different maintenance practices increase the uncertainty of BMP efficiency (Arhonditsis et al., 2019b, c; Liu et al., 2018).

Except from the mitigation of external loading, the complex interplay among instream physical (e.g., flow regimes, water temperature), chemical (e.g., adsorption/desorption), and biological (e.g., microbial decomposition) processes can profoundly modulate the ambient nutrient levels. In particular, sediment-water interfaces have been the research focus of the nutrient cycling in rivers, but recent evidence suggests that suspended particle water interfaces in the water column could also be hotspot of nutrient transformations (Xia et al., 2018). Suspended particles are key determinants in the transport, reactivity, and biological impacts of chemicals (Lin et al., 2021). For example, adsorption of dissolved phosphate onto inorganic particles, particularly amorphous iron oxyhydroxides, is considered a critical process to control bioavailable phosphate to relatively low levels (Pan et al., 2013). Depending on the reactivity of particles, there are critical thresholds of suspended matter concentrations below which water quality problems could become more severe, even if the exogenous nutrient loading

control is successful. Another interesting perspective of the tight coupling external loading-instream processes was recently offered by Tong et al. (2020), who argued that the growing imbalance between the rates of reduction of TN and TP external loading could lead to distinct differences in the nutrient stoichiometry (e.g., TN/TP ratios) of the receiving waterbodies and ultimately impact the risks of harmful algal blooms and broader ecosystem integrity.

A final note of consideration involves the granularity of the assessment of the progress of China's river water quality as we move forward. We advocate the assessment of the prevailing conditions using individual water quality snapshots based on samples collected regularly from different sites throughout the year, rather than any type of data aggregation in time and or space. The latter strategy may not be reflective of the wide range of spatiotemporal dynamics typically experienced in any riverine ecosystem nor does it allow us to evaluate our progress with ecosystem services at the degree of granularity required to assess the public sentiment. It would seem paradoxical to expect a single-valued average, reflective of the central tendency of multiple samples, to capture the degree of public satisfaction, which is often determined by the occurrence of water quality extremes (e.g., hypoxia leading to fish deaths, harmful algal blooms). Notably, while our delineation of the general trends based on yearly averages (or medians) painted a favourable picture regarding the riverine water quality in China, the reality is that excessively high pollutant concentrations are even frequently experienced, even in rivers that have demonstrably shown significant improvement (Figures S3 and S4). For example, more than 30% and 50% of the samples collected from all the sites across the Yellow River in 2018 registered $\text{NH}_3\text{-N}$ and PO_4 concentrations greater than 0.5 mg/L and 0.1 mg/L, respectively. Similar or even higher exceedance frequencies are still experienced in other rivers (Huai, Yangtze) with significant progress during our study period, which reinforces the point that China needs to intensify its nutrient management policies (Qin et al., 2020). The proposed assessment of the water quality status that revolves around extreme (or maximum allowable) pollutant levels has the conceptual advantage that not only tracks directly the actual incidences of water quality impairment, but is also closely connected with the targeted ecosystem services offered from riverine ecosystems (Arhonditsis et al., 2019a).

5. Conclusions

China's river water quality patterns and underlying covariates were characterized at a national scale to evaluate the recent progress and ongoing challenges in river management. Our analysis revealed a distinct water quality improvement with a gradual decrease in the frequency of prevalence of anoxic conditions, an alleviation of the severity of heavy metal pollution, and moderate success with the mitigation of cultural eutrophication during 2003–2018. River water quality is poorer in eastern China compared with that in western China. TP and $\text{NH}_3\text{-N}$ are collectively responsible for >85% of the identified incidences of impaired conditions. Our Bayesian modelling results revealed that the frequency of water quality impairments predominantly displays stronger relationships with anthropogenic covariates (82.5% for TP, 79.5% for $\text{NH}_3\text{-N}$) compared with natural factors (20.5% for TP, 17.5% for $\text{NH}_3\text{-N}$). Although considerable success was achieved in water quality restoration in China's rivers, it is still challenging to eradicate eutrophication and realize acceptable ecological conditions. The design of the remedial measures must be tailored to the site-specific landscape characteristics, meteorological conditions, and should also consider the increasing importance of non-point source pollution and internal nutrient loading.

Declaration of Competing Interest

The authors declare that they have no known competing financial interests or personal relationships that could have appeared to influence

the work reported in this paper.

Acknowledgments

This work was supported by Youth Innovation Promotion Association CAS (2019313 and 2017424), National Natural Science Foundation of China (41971138), the Strategic Priority Research Program of Chinese Academy of Sciences (XDA23020201) and Water Resources Science and Technology Program of Jiangsu, China (2019025, 2018003, 2020042 and 2020032). The authors would like to thank the National Tibetan Plateau Data Center for providing the meteorological data for our Bayesian modelling. Special thanks to Zeming Xu (Jilin Normal University, China), Shuai Zhang (Anhui Normal University, China) and Rui Qian (Northwest Normal University, China) for their technical support of our modelling exercise.

Supplementary materials

Supplementary material associated with this article can be found, in the online version, at doi:[10.1016/j.watres.2021.117309](https://doi.org/10.1016/j.watres.2021.117309).

References

- Arhonditsis, G.B., Neumann, A., Shimoda, Y., Javed, A., Blukacz-Richards, A., Mugalingam, S., 2019a. When can we declare a success? A Bayesian framework to assess the recovery rate of impaired freshwater ecosystems. *Environ. Int.* 130, 104821 <https://doi.org/10.1016/j.envint.2019.05.015>.
- Arhonditsis, G.B., Neumann, A., Shimoda, Y., Kim, D.-K., Dong, F., Onandia, G., Yang, C., Javed, A., Brady, M., Visha, A., Ni, F., Cheng, V., 2019b. Castles built on sand or predictive limnology in action? Part A: evaluation of an integrated modelling framework to guide adaptive management implementation in Lake Erie. *Ecol. Inform.* 53, 100968 <https://doi.org/10.1016/j.ecoinf.2019.05.014>.
- Arhonditsis, G.B., Neumann, A., Shimoda, Y., Kim, D.-K., Dong, F., Onandia, G., Yang, C., Javed, A., Brady, M., Visha, A., Ni, F., Cheng, V., 2019c. Castles built on sand or predictive limnology in action? Part B: designing the next monitoring-modelling-assessment cycle of adaptive management in Lake Erie. *Ecol. Inform.* 53, 100969 <https://doi.org/10.1016/j.ecoinf.2019.05.015>.
- Bouriga, M., Féron, O., 2013. Estimation of covariance matrices based on hierarchical inverse-Wishart priors. *J. Stat. Plan. Inference* 143 (4), 795–808. <https://doi.org/10.1016/j.jspi.2012.09.006>.
- Chen, X., Stokkal, M., Van Vliet, M.T.H., Stuijver, J., Wang, M., Bai, Z., Ma, L., Kroeze, C., 2019. Multi-scale modeling of nutrient pollution in the rivers of China. *Environ. Sci. Technol.* 53 (16), 9614–9625. <https://doi.org/10.1021/acs.est.8b07352>.
- Cui, Z., Zhang, H., Chen, X., Zhang, C., Ma, W., Huang, C., Zhang, W., Mi, G., Miao, Y., Li, X., Gao, Q., Yang, J., Wang, Z., Ye, Y., Guo, S., Lu, J., Huang, J., Lv, S., Sun, Y., Liu, Y., Peng, X., Ren, J., Li, S., Deng, X., Shi, X., Zhang, Q., Yang, Z., Tang, L., Wei, C., Jia, L., Zhang, J., He, M., Tong, Y., Tang, Q., Zhong, X., Liu, Z., Cao, N., Kou, C., Ying, H., Yin, Y., Jiao, X., Zhang, Q., Fan, M., Jiang, R., Zhang, F., Dou, Z., 2018. Pursuing sustainable productivity with millions of smallholder farmers. *Nature* 555 (7696), 363–366. <https://doi.org/10.1038/nature25785>.
- Ding, J., Jiang, Y., Liu, Q., Hou, Z., Liao, J., Fu, L., Peng, Q., 2016. Influences of the land use pattern on water quality in low-order streams of the Dongjiang River basin, China: a multi-scale analysis. *Sci. Total Environ.* 551–552, 205–216. <https://doi.org/10.1016/j.scitotenv.2016.01.162>.
- Du, S., Gu, H., Wen, J., Chen, K., Van Rompaey, A., 2015a. Detecting flood variations in Shanghai over 1949–2009 with Mann-Kendall tests and a newspaper-based database. *Water (Basel)* 7 (5). <https://doi.org/10.3390/w7051808>.
- Du, S., Shi, P., Van Rompaey, A., Wen, J., 2015b. Quantifying the impact of impervious surface location on flood peak discharge in urban areas. *Nat. Hazards* 76 (3), 1457–1471. <https://doi.org/10.1007/s11069-014-1463-2>.
- Green, M.B., Nieber, J.L., Johnson, G., Magner, J., Schaefer, B., 2007. Flow path influence on an N: P ratio in two headwater streams: a paired watershed study. *J. Geophys. Res.-Biogeosci.* 112 (G3), G03015. <https://doi.org/10.1029/2007jg004043>.
- Grill, G., Lehner, B., Thieme, M., Geenen, B., Tickner, D., Antonelli, F., Babu, S., Borrelli, P., Cheng, L., Crochetiere, H., Ehalt Macedo, H., Filgueiras, R., Goichot, M., Higgins, J., Hogan, Z., Lip, B., McClain, M.E., Meng, J., Mulligan, M., Nilsson, C., Olden, J.D., Opperman, J.J., Petry, P., Reidy Liermann, C., Sáenz, L., Salinas-Rodríguez, S., Schelle, P., Schmitt, R.J.P., Snider, J., Tan, F., Tockner, K., Valdujo, P. H., van Soesbergen, A., Zarfl, C., 2019. Mapping the world's free-flowing rivers. *Nature* 569 (7755), 215–221. <https://doi.org/10.1038/s41586-019-1111-9>.
- He, J., Yang, K., Tang, W., Lu, H., Qin, J., Chen, Y., Li, X., 2020. The first high-resolution meteorological forcing dataset for land process studies over China. *Sci. Data* 7 (1), 25. <https://doi.org/10.1038/s41597-020-0369-y>.
- Huang, J., Zhang, Y., Arhonditsis, G.B., Gao, J., Chen, Q., Wu, N., Dong, F., Shi, W., 2019. How successful are the restoration efforts of China's lakes and reservoirs? *Environ. Int.* 123, 96–103. <https://doi.org/10.1016/j.envint.2018.11.048>.
- Jarvis, H.P., Smith, D.R., Norton, L.R., Edwards, F.K., Bowes, M.J., King, S.M., Scarlett, P., Davies, S., Dils, R.M., Bachiller-Jareno, N., 2018. Phosphorus and

- nitrogen limitation and impairment of headwater streams relative to rivers in Great Britain: a national perspective on eutrophication. *Sci. Total Environ.* 621, 849–862. <https://doi.org/10.1016/j.scitotenv.2017.11.128>.
- Jiang, Y., Zevenbergen, C., Ma, Y., 2018. Urban pluvial flooding and stormwater management: a contemporary review of China's challenges and "sponge cities" strategy. *Environ. Sci. Policy* 80, 132–143. <https://doi.org/10.1016/j.envsci.2017.11.016>.
- Lebreton, L.C.M., Van der Zwet, J., Damsteeg, J.W., Slat, B., Andrady, A., Reisser, J., 2017. River plastic emissions to the world's oceans. *Nat. Commun.* 8, 10. <https://doi.org/10.1038/ncomms15611>.
- Lehner, B., Liermann, C.R., Revenga, C., Vörösmarty, C., Fekete, B., Crouzet, P., Döll, P., Endejan, M., Frenken, K., Magome, J., Nilsson, C., Robertson, J.C., Rödel, R., Sindorf, N., Wissler, D., 2011. High-resolution mapping of the world's reservoirs and dams for sustainable river-flow management. *Front. Ecol. Environ.* 9 (9), 494–502. <https://doi.org/10.1890/100125>.
- Li, G.C., Xia, X.H., Yang, Z.F., Wang, R., Voulvoulis, N., 2006. Distribution and sources of polycyclic aromatic hydrocarbons in the middle and lower reaches of the Yellow River. *China. Environ. Pollut.* 144 (3), 985–993. <https://doi.org/10.1016/j.envpol.2006.01.047>.
- Li, S., Shi, W., Liu, W., Li, H., Zhang, W., Hu, J., Ke, Y., Sun, W., Ni, J., 2018. A duodecennial national synthesis of antibiotics in China's major rivers and seas (2005–2016). *Sci. Total Environ.* 615, 906–917. <https://doi.org/10.1016/j.scitotenv.2017.09.328>.
- Lin, H., Xia, X., Zhang, Q., Zhai, Y., Wang, H., 2021. Can the hydrophobic organic contaminants in the filtrate passing through 0.45µm filter membranes reflect the water quality? *Sci. Total Environ.* 752, 141916 <https://doi.org/10.1016/j.scitotenv.2020.141916>.
- Liu, X., Sheng, H., Jiang, S., Yuan, Z., Zhang, C., Elser, J.J., 2016. Intensification of phosphorus cycling in China since the 1600s. *Proc. Natl. Acad. Sci.* 113 (10), 2609–2614. <https://doi.org/10.1073/pnas.1519554113>.
- Liu, Y., Engel, B.A., Flanagan, D.C., Gitau, M.W., McMillan, S.K., Chaubey, I., Singh, S., 2018. Modeling framework for representing long-term effectiveness of best management practices in addressing hydrology and water quality problems: framework development and demonstration using a Bayesian method. *J. Hydrol.* 560, 530–545. <https://doi.org/10.1016/j.jhydrol.2018.03.053>.
- Liu, Y., Fang, F., Li, Y., 2014. Key issues of land use in China and implications for policy making. *Land Use Policy* 40, 6–12. <https://doi.org/10.1016/j.landusepol.2013.03.013>.
- Liu, Y., Wang, Y., 2016. Exploring the integrated planning of city drainage and waterlogging prevention based on Sponge City idea: the case of Badali district in Tianjin (In Chinese). *City* 4, 54–59.
- Liu, Y.S., Li, Y.H., 2017. Revitalize the world's countryside. *Nature* 548 (7667), 275–277. <https://doi.org/10.1038/548275a>.
- Long, T., Wellen, C., Arhonditsis, G., Boyd, D., 2014. Evaluation of stormwater and snowmelt inputs, land use and seasonality on nutrient dynamics in the watersheds of Hamilton Harbour, Ontario, Canada. *J. Gt. Lakes Res.* 40 (4), 964–979. <https://doi.org/10.1016/j.jglr.2014.09.017>.
- Long, T., Wellen, C., Arhonditsis, G., Boyd, D., Mohamed, M., O'Connor, K., 2015. Estimation of tributary total phosphorus loads to Hamilton Harbour, Ontario, Canada, using a series of regression equations. *J. Gt. Lakes Res.* 41 (3), 780–793. <https://doi.org/10.1016/j.jglr.2015.04.001>.
- Maavara, T., Chen, Q., Van Meter, K., Brown, L.E., Zhang, J., Ni, J., Zarfl, C., 2020. River dam impacts on biogeochemical cycling. *Nat. Rev. Earth Environ.* 1 (2), 103–116. <https://doi.org/10.1038/s43017-019-0019-0>.
- Maavara, T., Parsons, C.T., Ridenour, C., Stojanovic, S., Dürr, H.H., Powley, H.R., Van Cappellen, P., 2015. Global phosphorus retention by river damming. *Proc. Natl. Acad. Sci.* 112 (51), 15603–15608. <https://doi.org/10.1073/pnas.1511797112>.
- Mallows, C.L., 2000. Some comments on C-P. *Technometrics* 42 (1), 87–94. <https://doi.org/10.2307/1271437>.
- Messenger, M.L., Lehner, B., Grill, G., Nedeva, I., Schmitt, O., 2016. Estimating the volume and age of water stored in global lakes using a geo-statistical approach. *Nat. Commun.* 7, 13603. <https://doi.org/10.1038/ncomms13603>.
- Oki, T., Kanae, S., 2006. Global hydrological cycles and world water resources. *Science* 313 (5790), 1068–1072. <https://doi.org/10.1126/science.1128845>.
- Ongley, E.D., Zhang, X., Yu, T., 2010. Current status of agricultural and rural non-point source Pollution assessment in China. *Environ. Pollut.* 158 (5), 1159–1168. <https://doi.org/10.1016/j.envpol.2009.10.047>.
- Palmer, M., Ruhi, A., 2019. Linkages between flow regime, biota, and ecosystem processes: implications for river restoration. *Science* 365 (6459), eaaw2087. <https://doi.org/10.1126/science.aaw2087>.
- Pan, G., Krom, M.D., Zhang, M.Y., Zhang, X.W., Wang, L.J., Dai, L.C., Sheng, Y.Q., Mortimer, R.J.G., 2013. Impact of suspended inorganic particles on phosphorus cycling in the Yellow River (China). *Environ. Sci. Technol.* 47 (17), 9685–9692. <https://doi.org/10.1021/es4005619>.
- Plummer, M., 2006. Comment on article by Celeux et al. *Bayesian Anal.* 1 (4), 681–686. <https://doi.org/10.1214/06-BA122C>.
- Powers, S.M., Brullesma, T.W., Burt, T.P., Chan, N.I., Elser, J.J., Haygarth, P.M., Howden, N.J.K., Jarvie, H.P., Lyu, Y., Peterson, H.M., Sharpley, A.N., Shen, J., Worrall, F., Zhang, F., 2016. Long-term accumulation and transport of anthropogenic phosphorus in three river basins. *Nat. Geosci.* 9, 353. <https://doi.org/10.1038/ngeo2693>.
- Qin, B., Zhang, Y., Zhu, G., Gong, Z., Deng, J., Hamilton, D.P., Gao, G., Shi, K., Zhou, J., Shao, K., Zhu, M., Zhou, Y., Tang, X., Li, L., 2020. Are nitrogen-to-phosphorus ratios of Chinese lakes actually increasing? *Proc. Natl. Acad. Sci.* 117 (35), 21000–21002. <https://doi.org/10.1073/pnas.2013445117>.
- Qu, H.J., Kroeze, C., 2010. Past and future trends in nutrients export by rivers to the coastal waters of China. *Sci. Total Environ.* 408 (9), 2075–2086. <https://doi.org/10.1016/j.scitotenv.2009.12.015>.
- Qu, J., Wang, H., Wang, K., Yu, G., Ke, B., Yu, H., Ren, H., Zheng, X., Li, J., Li, W., Gao, S., Gong, H., 2019. Municipal wastewater treatment in China: development history and future perspectives. *Front. Environ. Sci. Eng.* 13 (6), 88. <https://doi.org/10.1007/s11783-019-1172-x>.
- Shen, Z., Liao, Q., Hong, Q., Gong, Y., 2012. An overview of research on agricultural non-point source pollution modelling in China. *Sep. Purif. Technol.* 84, 104–111. <https://doi.org/10.1016/j.seppur.2011.01.018>.
- Singh, R., Singh, A.P., Kumar, S., Giri, B.S., Kim, K.-H., 2019. Antibiotic resistance in major rivers in the world: a systematic review on occurrence, emergence, and management strategies. *J. Clean. Prod.* 234, 1484–1505. <https://doi.org/10.1016/j.jclepro.2019.06.243>.
- Stockwell, J.D., Doubek, J.P., Adrian, R., Anneville, O., Carey, C.C., Carvalho, L., De Senerpont Domis, L.N., Dur, G., Frassl, M.A., Grossart, H.-P., Ibelings, B.W., Lajeunesse, M.J., Lewandowska, A.M., Llamas, M.E., Matsuzaki, S.-I.S., Nodine, E.R., Nöges, P., Patil, V.P., Pomati, F., Rinke, K., Rudstam, L.G., Rusak, J.A., Salmaso, N., Seltmann, C.T., Straile, D., Thackeray, S.J., Thiery, W., Urrutia-Cordero, P., Venail, P., Verburg, P., Woolway, R.I., Zohary, T., Andersen, M.R., Bhattacharya, R., Hejzlar, J., Janatian, N., Kpodonu, A.T.N.K., Williamson, T.J., Wilson, H.L., 2020. Storm impacts on phytoplankton community dynamics in lakes. *Glob. Change Biol.* 26 (5), 2756–2784. <https://doi.org/10.1111/gcb.15033>.
- Strokal, M., Ma, L., Bai, Z., Luan, S., Kroeze, C., Oenema, O., Velthof, G., Zhang, F., 2016. Alarming nutrient pollution of Chinese rivers as a result of agricultural transitions. *Environ. Res. Lett.* 11 (2), 024014 <https://doi.org/10.1088/1748-9326/11/2/024014>.
- Tao, T., Xin, K., 2014. A sustainable plan for China's drinking water: tackling pollution and using different grades of water for different tasks is more efficient than making all water potable. *Nature* 511 (7511), 527–529. <https://doi.org/10.1038/511527a>.
- The Ministry of Ecology and Environment, P.R.C., 2020a. Annual Bulletin of China's Ecology and Environment. <http://www.cnemc.cn/jcgb/zghjzkgb/>.
- The Ministry of Ecology and Environment, P.R.C., 2020b. Second National Pollutant Source Census Bulletin. http://www.mee.gov.cn/xxgk2018/xxgk/xxgk01/202006/t20200610_783547.html.
- Tong, Y., Wang, M., Peñuelas, J., Liu, X., Paerl, H.W., Elser, J.J., Sardans, J., Couture, R.-M., Larssen, T., Hu, H., Dong, X., He, W., Zhang, W., Wang, X., Zhang, Y., Liu, Y., Zeng, S., Kong, X., Janssen, A.B.G., Lin, Y., 2020. Improvement in municipal wastewater treatment alters lake nitrogen to phosphorus ratios in populated regions. *Proc. Natl. Acad. Sci.* 117 (21), 11566–11572. <https://doi.org/10.1073/pnas.1920759117>.
- United Nations, 2020. <https://www.un.org/sustainabledevelopment/water-and-sanitation/>.
- van Vliet, M.T.H., Franssen, W.H.P., Yearsley, J.R., Ludwig, F., Haddeland, I., Lettenmaier, D.P., Kabat, P., 2013. Global river discharge and water temperature under climate change. *Glob. Environ. Change-Human Policy Dimens.* 23 (2), 450–464. <https://doi.org/10.1016/j.gloenvcha.2012.11.002>.
- Vehtari, A., Gelman, A., Simpson, D., Carpenter, B., Bürkner, P.-C., 2020. Rank-normalization, folding, and localization: an improved R for assessing convergence of MCMC. *Bayesian Anal.* <https://doi.org/10.1214/20-BA1221>.
- Vörösmarty, C.J., McIntyre, P.B., Gessner, M.O., Dudgeon, D., Prusevich, A., Green, P., Glidden, S., Bunn, S.E., Sullivan, C.A., Liermann, C.R., Davies, P.M., 2010. Global threats to human water security and river biodiversity. *Nature* 467 (7315), 555–561. <https://doi.org/10.1038/nature09440>.
- Wang, S.A., Fu, B.J., Piao, S.L., Lu, Y.H., Ciais, P., Feng, X.M., Wang, Y.F., 2016. Reduced sediment transport in the Yellow River due to anthropogenic changes. *Nat. Geosci.* 9 (1), 38–42. <https://doi.org/10.1038/ngeo2602>.
- Wang, Y., Ni, J., Yue, Y., Li, J., Borthwick, A.G.L., Cai, X., Xue, A., Li, L., Wang, G., 2019. Solving the mystery of vanishing rivers in China. *Natl. Sci. Rev.* 6 (6), 1239–1246. <https://doi.org/10.1093/nsr/nwz022>.
- Withers, P.J.A., Sylvester-Bradley, R., Jones, D.L., Healey, J.R., Talboys, P.J., 2014. Feed the crop not the soil: rethinking phosphorus management in the food chain. *Environ. Sci. Technol.* 48 (12), 6523–6530. <https://doi.org/10.1021/es501670j>.
- Xia, X., Zhang, S., Li, S., Zhang, L., Wang, G., Zhang, L., Wang, J., Li, Z., 2018. The cycle of nitrogen in river systems: sources, transformation, and flux. *Environ. Sci.* 20 (6), 863–891. <https://doi.org/10.1039/C8EM00042E>.
- Xiao, R., Wang, G., Zhang, Q., Zhang, Z., 2016. Multi-scale analysis of relationship between landscape pattern and urban river water quality in different seasons. *Sci Rep* 6, 25250. <https://doi.org/10.1038/srep25250>.
- Yang, C., Yang, P., Geng, J., Yin, H., Chen, K., 2020. Sediment internal nutrient loading in the most polluted area of a shallow eutrophic lake (Lake Chaohu, China) and its contribution to lake eutrophication. *Environ. Pollut.* 262, 114292 <https://doi.org/10.1016/j.envpol.2020.114292>.
- Yang, X., Jomaa, S., Büttner, O., Rode, M., 2019. Autotrophic nitrate uptake in river networks: a modeling approach using continuous high-frequency data. *Water Res.* 157, 258–268. <https://doi.org/10.1016/j.watres.2019.02.059>.
- Yi, Q., Chen, Q., Hu, L., Shi, W., 2017. Tracking nitrogen sources, transformation, and transport at a basin scale with complex plain river networks. *Environ. Sci. Technol.* 51 (10), 5396–5403. <https://doi.org/10.1021/acs.est.6b06278>.
- Zhang, Q.Q., Ying, G.G., Pan, C.G., Liu, Y.S., Zhao, J.L., 2015. Comprehensive evaluation of antibiotics emission and fate in the River Basins of China: source analysis, multimedia modeling, and linkage to bacterial resistance. *Environ. Sci. Technol.* 49 (11), 6772–6782. <https://doi.org/10.1021/acs.est.5b00729>.
- Zhou, X., Li, Z., Zheng, T., Yan, Y., Li, P., Odey, E.A., Mang, H.P., Uddin, S.M.N., 2018. Review of global sanitation development. *Environ. Int.* 120, 246–261. <https://doi.org/10.1016/j.envint.2018.07.047>.